Title
Effects of stereochemistry, saturation, and hydrocarbon chain length on the ability of synthetic constrained azacyclic sphingolipids to trigger nutrient transporter down-regulation, vacuolation, and cell death.

Journal
Bioorganic & medicinal chemistry, 24(18)

ISSN
0968-0896

Authors
Perryman, Michael S
Tessier, Jérémie
Wiher, Timothy
et al.

Publication Date
2016-09-01

DOI
10.1016/j.bmc.2016.07.038

Bioorganic & Medicinal Chemistry 24 (2016) 4390–4397

Contents lists available at ScienceDirect

Bioorganic & Medicinal Chemistry

journal homepage: www.elsevier.com/locate/bmc

Effects of stereochemistry, saturation, and hydrocarbon chain length on the ability of synthetic constrained azacyclic sphingolipids to trigger nutrient transporter down-regulation, vacuolation, and cell death

Michael S. Perryman [a], Jérémie Tessier [a], Timothy Wiher [b], Heather O'Donoghue [a], Alison N. McCracken [b], Seong M. Kim [b], Dean G. Nguyen [b], Grigor S. Simitian [b], Matheus Viana [b], Susanne Rafelski [b], Aimee L. Edinger [b,*], Stephen Hanessian [a,*]

[a] Department of Chemistry, Université de Montréal, PO Box 6128, Station Centre-Ville, Montréal, QC H3C 3J7, Canada
[b] Department of Developmental and Cell Biology, University of California, Irvine, 2128 Natural Sciences 1, CA 92697-2300, USA

ARTICLE INFO

Article history:
Received 13 June 2016
Revised 13 July 2016
Accepted 16 July 2016
Available online 18 July 2016

Keywords:
FTY720
Nutrient transporter loss
Azacycles
Sphingolipids
Ceramides

ABSTRACT

Constrained analogs containing a 2-hydroxymethylpyrrolidine core of the natural sphingolipids sphingosine, sphinganine, *N*,*N*-dimethylsphingosine and *N*-acetyl variants of sphingosine and sphinganine (C_2-ceramide and dihydro-C_2-ceramide) were synthesized and evaluated for their ability to down-regulate nutrient transporter proteins and trigger cytoplasmic vacuolation in mammalian cells. In cancer cells, the disruptions in intracellular trafficking produced by these sphingolipids lead to cancer cell death by starvation. Structure activity studies were conducted by varying the length of the hydrocarbon chain, the degree of unsaturation and the presence or absence of an aryl moiety on the appended chains, and stereochemistry at two stereogenic centers. In general, cytotoxicity was positively correlated with nutrient transporter down-regulation and vacuolation. This study was intended to identify structural and functional features in lead compounds that best contribute to potency, and to develop chemical biology tools that could be used to isolate the different protein targets responsible for nutrient transporter loss and cytoplasmic vacuolation. A molecule that produces maximal vacuolation and transporter loss is expected to have the maximal anti-cancer activity and would be a lead compound.

1. Introduction

Sphingolipids are evolutionarily conserved regulators of nutrient access. Under heat stress, yeast produce the sphingolipid phytosphingosine thereby triggering nutrient permease internalization that starves cells into an adaptive proliferative arrest.[1,2] In mammalian cells, the related sphingolipid ceramide is generated under a variety of stress stimuli and also triggers nutrient transporter down-regulation that induces a starvation-like phenotype.[3–5] The FDA approved sphingolipid drug FTY720 (**1**) produces similar nutrient transporter loss in both yeast and mammalian cells.[6,7] Remarkably, FTY720, phytosphingosine, and nutrient restriction produce largely overlapping transcriptional responses in yeast.[2] Together, these studies suggest that sphingolipids act as evolutionarily conserved starvation mimetics that exert their effects by down-regulating cell surface transporters for amino acids and glucose.

Tumor cells increase nutrient transporter expression and up-regulate anabolic pathways to support their uncontrolled growth.[3] Although accelerated nutrient uptake allows non-homeostatic proliferation, the constitutive demand for metabolic substrates in cancer cells becomes a liability under nutrient limiting conditions. When extracellular nutrients are scarce, normal cells: (1) switch to more efficient metabolic programs (e.g., reduce glycolysis and increase oxidative phosphorylation), (2) decrease nutrient demand by slowing proliferation, and (3) increase catabolic processes to generate nutrients from intracellular sources. The constitutive activation of oncogenes and the loss of the tumor suppressor proteins limits all three of these adaptive responses, sensitizing cancer cells to nutrient limitation. Like bears that fail to hibernate in the winter, cancer cells die under nutrient stress that causes normal cells to become quiescent.[8–10] The differential sensitivity of normal

* Corresponding authors.
E-mail addresses: aedinger@uci.edu (A.L. Edinger), stephen.hanessian@umontreal.ca (S. Hanessian).

http://dx.doi.org/10.1016/j.bmc.2016.07.038
0968-0896/

and transformed cells to nutrient stress suggests that sphingolipids that induce starvation by down-regulating nutrient transporters may have therapeutic value as selective anti-cancer agents.[3]

Consistent with this proposal, FTY720 (**1**) has striking activity against both solid tumors and hematologic malignancies in animal models.[6,11–15] Although FTY720 (**1**) is an FDA-approved immunosuppressant that is both water soluble and orally bioavailable, it cannot be repurposed as a cancer therapy because it triggers profound bradycardia due to activation of sphingosine-1-phosphate (S1P) receptors at the elevated anti-cancer dose.[16–19] We have developed constrained FTY720 analogs based on a pyrrolidine core structure to eliminate S1P receptor activation while retaining anti-cancer effects.[13,20,21] These pyrrolidine analogs exemplified by the enantiomeric pairs, **2** and **3** as well as **4** and **5** (Fig. 1), retain FTY720's water solubility, oral bioavailability, and anti-tumor activity but no longer trigger bradycardia.[13,20,22,23] While these previously reported compounds are effective in animal models and were found to accumulate in tumors[13,22], their low micromolar potency (IC_{50} of 2–5 μM) warranted a study of structural and functional features within a pyrrolidine core that might lead to an improved activity profile.

We have previously linked the anti-neoplastic activity of FTY720 and its pyrrolidine analogs to their ability to trigger nutrient transporter loss.[6,13,20] More recently, we have shown that these compounds also produce cytosolic vacuolation that contributes to their anti-neoplastic effects in vitro and in vivo.[22] These vacuoles primarily represent the multivesicular body, a pre-lysosomal compartment of the cell that swells when endocytic cargo is no longer transferred to the lysosome for degradation. Both transporter down-regulation and vacuolation depend on the activation of protein phosphatase 2A (PP2A).[6,13,22] These pyrrolidine FTY720 analogs are somewhat unusual in that they activate the putative target rather than inhibit its function. However, the endogenous sphingolipid C_2-ceramide (**9**) increases the phosphatase activity of purified, recombinant PP2A catalytic subunit in in vitro assays suggesting that sphingolipids may bind to an allosteric regulatory site that promotes enzyme activation.[22,24,25] The micromolar IC_{50} of ceramide in these assays is consistent with its role as an allosteric activator of PP2A given that cellular sphingolipid concentrations are in this range. This activation is specific as the closely related compound, dihydro-C_2-ceramide (**10**), fails to activate PP2A. The synthetic sphingolipid FTY720 (**1**) and dimethylsphingosine (**8**) also activate PP2A but with 10- to 20-fold higher potency, and photo-affinity labeling probes derived from sphingosine (**6**) isolate PP2A subunits [15,22,26,27 reviewed in[28,29]]. Interestingly, while both ceramide and FTY720 analogs trigger PP2A-dependent nutrient transporter loss, ceramide fails to produce the vacuolation seen with FTY720.[4,6,22] PP2A is a heterotrimeric complex.[30] There are multiple isoforms of each PP2A subunit in cells, including more than 15 isoforms of the regulatory subunit that controls substrate specificity. Because PP2A inhibitors block both transporter loss and vacuolation, we propose that two distinct PP2A complexes are activated by FTY720 to induce these phenotypes: one PP2A complex that induces nutrient transporter loss is also activated by ceramide while a second complex responsible for vacuolation is uniquely activated by FTY720 (Supplemental information). Given the biological complexity of PP2A, the value of developing chemical biology tools that could selectively isolate the sphingolipid-activated PP2A complexes responsible for either transporter loss or vacuolation is readily apparent.

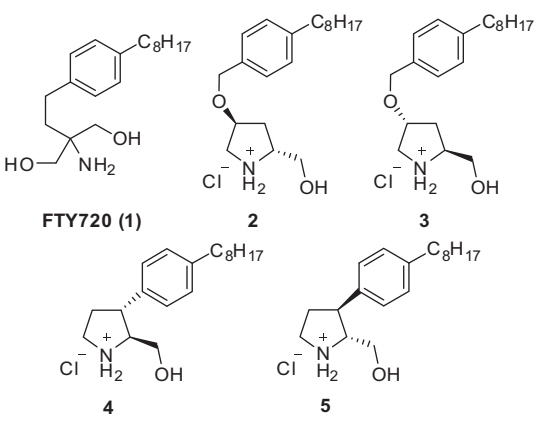

Figure 1. Structures of FTY720 (**1**, Gilenya) and constrained analogs, **2**–**5**.

We have previously described two distinct series of FTY720 analogs with anti-cancer activity based on either *C*-aryl substituted pyrrolidine analogs such as **4** and **5**[13], or more synthetically accessible *O*-benzyl substituted pyrrolidine analogs such as **2** and **3**[20] (Fig. 1). Interestingly, conformationally constraining the flexible aminodiol portion of FTY720 (**1**) as in the above mentioned analogs eliminated undesirable S1P receptor activity.[13,20,23] Intrigued by the differential ability of C_2-ceramide (**9**) and dihydro-C_2-ceramide (**10**) to activate PP2A and kill cells[22,24,31], we set out to prepare constrained analogs of the aminodiol portion of natural sphingolipids with the goals of identifying structural features important for the transporter loss, vacuolation, and cytotoxicity induced by FTY720 (**1**). We adopted the same strategy of conformational constraint to generate pyrrolidine analogs of sphingosine (**6**), sphinganine (**7**), dimethylsphingosine (**8**), and the *N*-acetylated analogs **9** and **10**, by varying the length of the alkyl chain, the degree of unsaturation and the absolute stereochemistry (Fig. 2).

2. Results and discussion

While our initial evaluations of constrained FTY720 analogs assessed their ability to kill cells and trigger nutrient transporter down-regulation[13,20], further study has revealed that the compounds also disrupt late endocytic trafficking, producing profound cytoplasmic vacuolation[22] (Fig. 3).

As both transporter loss[6] and vacuolation[22] contribute to anti-cancer activity, our structure activity relationship studies evaluated both phenotypes. Nutrient transporter down-regulation was monitored by quantifying surface levels of the amino acid transporter-associated protein, CD98, by flow cytometry. To compare vacuolation, a semi-quantitative assay was developed. This quantification strategy is described in detail in the Supplementary methods. Using this method, a vacuolation score was produced that ranged from 0 to 84 and corresponded to roughly two times the percent of the cytosol that contained vacuoles (Supplementary Figs. S1–S3). The concentration that killed half the cells at 48 h (IC_{50}) was determined by measuring vital dye exclusion, a more stringent assay than the higher throughput MTT or Cell Titer Glo assays in which cytostatic compounds score as well as cytotoxic agents. The murine hematopoietic cell line FL5.12 was selected for these studies because these cells exhibit robust nutrient transporter loss and vacuolation providing a large dynamic range that would facilitate comparing compounds.

Our SAR strategy was founded on results obtained with the naturally occurring sphingolipids sphingosine (**6**) and sphinganine (**7**) and the moderately soluble, short-chain C_2-ceramide (**9**) and dihydro-C_2-ceramide (**10**) that are often used in place of extremely hydrophobic (but physiologic) long-chain ceramides (Figs. 2 and 3). Sphingosine (**6**) and sphinganine (**7**) both triggered nutrient transporter loss and vacuolation and efficiently killed cells with IC_{50}'s of 3.6 and 3.5 μM, respectively (Fig. 3 and Table 1). C_2-Ceramide (**9**) triggered nutrient transporter loss with reduced potency compared to sphingosine (**6**) since 50 μM C_2-ceramide (**9**) was required to cause similar transporter loss as 2.5 μM sphingosine

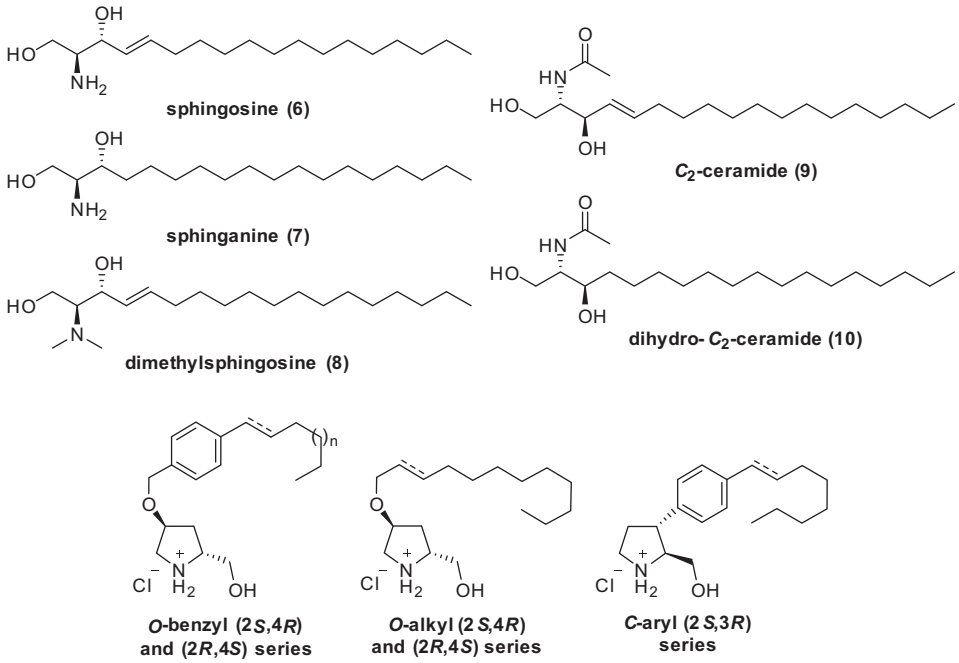

Figure 2. Structures of sphingolipids and pyrrolidine analogs.

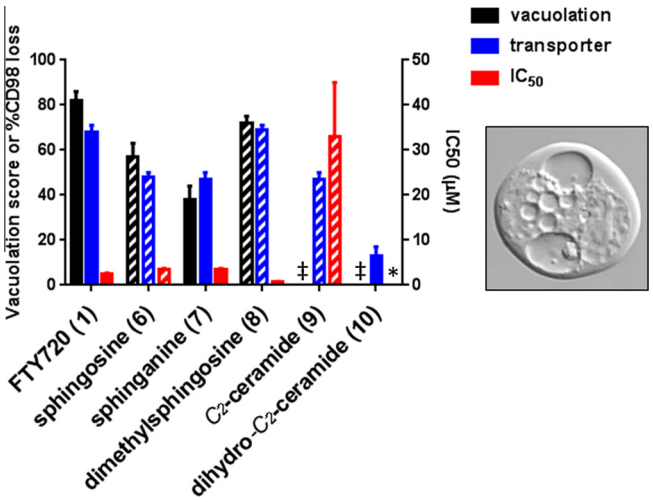

Figure 3. Effects of FTY720 and natural sphingolipids on vacuolation, transporter loss, and IC_{50}. In vacuolation and transporter assays, compounds **1** and **6**–**8** were tested at 2.5 μM while **9** and **10** were used at 50 μM. Unsaturated sphingolipids are shown with hatched bars. Mean values are presented +/− SEM for transporter loss and vacuolation and with 95% CI for IC_{50}'s. ‡, no vacuolation detected; ∗, not determined as the IC_{50} for dihydro-C_2-ceramide (**10**) was not reached at 50 μM, the limit of its solubility in cell culture medium. A vacuolated FL5.12 cell is shown; a complete description of how vacuolation was scored is available in the Supplementary information.

(**6**) (Table 1, entries 2 and 5). C_2-Ceramide did not cause vacuolation at any dose. Consistent with previous reports that it does not activate PP2A[22,24], dihydro-C_2-ceramide (**10**) failed to kill cells, did not efficiently trigger CD98 down-regulation, and caused no vacuolation (Table 1, entry 6 and Fig. 3). While C_2-ceramide (**9**) was much less active than sphingosine (**6**), dimethylsphingosine (**8**) was almost 5-fold more potent (IC_{50} = 0.77 μM) (Table 1, entry 4 and Fig. 3). It is of interest that saturation of sphingosine reduced vacuolation while transporter loss and cytotoxicity were unaffected. The activity profile of these natural sphingolipids led us to investigate pyrrolidine analogs containing *O*-benzyl and *C*-aryl tethered hydrocarbon chains by altering the length and degree of unsaturation of the hydrocarbon chain and derivatizing the amine group. The results are included in Tables 1–3 and Figures 4–6.

The hydrocarbon tail of FTY720 (**1**) and of our constrained *O*-benzyl analogs **2** and **3** is shorter (C8) than that present in sphingosine (**6**, C12), although the aromatic group in FTY720 (**1**) extends the hydrophobic region (Fig. 2). To determine whether the chain length of the *O*-benzyl pyrrolidine FTY720 analogs **2** and **3** was optimized for transporter loss and vacuolation, we generated compounds in this series with C6, C8, C10, C12, or C14 hydrocarbon chains (Fig. 2, Table 1). In both stereochemical series, (2*R*,4*S*) and (2*S*,4*R*), analogs **14** (C12), **16** (C14), **21** (C12), and **23** (C14) that bear a fully saturated chain lost activity in transporter and vacuolation assays (Fig. 4, Table 1, entries 11, 13, 19, and 21). When the hydrocarbon chain was partially unsaturated, as in **15** (C12) and **22** (C12), the longer chain was tolerated (Table 1 entries 12 and 20). The finding that C12 analogs are more active when unsaturated in both stereochemical series as represented by **14** and **15** and the enantiomeric **21** and **22**, respectively (entries 11, 12, 19, and 20), suggests that introducing a double bond may permit a better fit of the suboptimally long hydrocarbon chain in a hydrophobic binding site in the target protein. We recall that sphingosine (**6**) was better at vacuolation than its saturated congener sphinganine (**7**) (Table 1, entries 2 and 3).

A C14 chain was not tolerated in vacuolation assays and reduced transporter down-regulation even when unsaturated (**17** and **24**, Table 1 entries 14 and 22). Analogs in this *O*-benzyl series with shorter C6 hydrocarbon chains (**11**, **12** and **18**, Table 1 entries 7, 8 and 15, respectively) were also less active than the saturated and unsaturated C8 counterparts, (**2**, **3**, **13** and **19**, (Table 1, entries 9, 16, 10 and 17, respectively) leading to less transporter down-regulation and no vacuolation. These results indicate that a C8 hydrocarbon chain length in this series leads to optimal potency in both transporter and vacuolation assays, although a C12 chain as in **15** and **22**, is tolerated provided that the chain is partially unsaturated (Table 1, entries 12 and 20).

Interestingly, in the unsaturated (2*S*,4*R*) series corresponding to **3**, peak vacuolation scores were higher than peak transporter loss scores, while in the unsaturated (2*R*,4*S*) series corresponding to

Table 1
Comparison of activities of *O*-benzyl and *C*-aryl pyrrolidine analogs

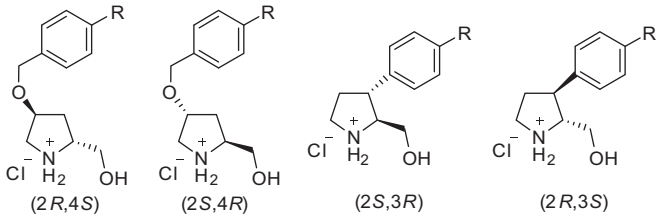

Entry	Compound; Stereochemistry	R	Compound number	IC_{50} (μM) [95% CI]	%CD98 down-regulation	Vacuolation score
1	FTY720		**1**	2.4 [2.1–2.7]	68 ± 3	82 ± 4
2	Sphingosine		**6**	3.6 [3.5–3.7]	48 ± 2	57 ± 6
3	Sphinganine		**7**	3.5 [3.3–3.7]	47 ± 3	38 ± 6
4	Dimethylsphingosine		**8**	0.8 [0.7–0.9]	69 ± 2	72 ± 3
5	C_2-Ceramide		**9**	33.0 [23.3–47.0]	47 ± 3	0
6	Dihydro-C_2-ceramide		**10**	Cytostatic	13 ± 4	0
	O-Benzyl series					
7	(2*R*,4*S*)	C_6H_{13}	**11**	2.7 [2.6-2.8]	30 ± 2	0
8	(2*R*,4*S*)	C_6H_{11}	**12**	5.5 [5.3–5.7]	30 ± 4	0
9	(2*R*,4*S*)	C_8H_{17}	**2**	2.0 [1.8-2.2]	63 ± 3	33 ± 2
10	(2*R*,4*S*)	C_8H_{15}	**13**	1.4 [1.3-1.6]	64 ± 1	27 ± 1
11	(2*R*,4*S*)	$C_{12}H_{25}$	**14**	10.1 [8.7–11.6]	13 ± 3	3 ± 1
12	(2*R*,4*S*)	$C_{12}H_{23}$	**15**	2.8 [2.4–3.3]	52 ± 1	33 ± 3
13	(2*R*,4*S*)	$C_{14}H_{29}$	**16**	10.5 [9.7–11.3]	12 ± 3	4 ± 2
14	(2*R*,4*S*)	$C_{14}H_{27}$	**17**	5.1 [5.0–5.3]	19 ± 3	8 ± 1
15	(2*S*,4*R*)	C_6H_{11}	**18**	5.7 [3.9–8.3]	9 ± 3	5 ± 2
16	(2*S*,4*R*)	C_8H_{17}	**3**	3.0 [2.9-3.2]	48 ± 2	47 ± 2
17	(2*S*,4*R*)	C_8H_{15}	**19**	2.4 [2.3–2.4]	41 ± 3	70 ± 1
18	(2*S*,4*R*)	$C_{10}H_{21}$	**20**	3.6 [3.4–3.7]	28 ± 1	36 ± 5
19	(2*S*,4*R*)	$C_{12}H_{25}$	**21**	3.9 [3.7–4.2]	14 ± 4	30 ± 2
20	(2*S*,4*R*)	$C_{12}H_{23}$	**22**	2.4 [2.3–2.5]	40 ± 2	76 ± 6
21	(2*S*,4*R*)	$C_{14}H_{29}$	**23**	5.7 [5.5–5.9]	19 ± 1	3 ± 3
22	(2*S*,4*R*)	$C_{14}H_{27}$	**24**	7.3 [6.7–8.1]	20 ± 3	1 ± 1
	C-Aryl series					
23	(2*S*,3*R*)	C_8H_{17}	**4**	1.9 [1.8-2.1]	54 ± 1	81 ± 3
24	(2*S*,3*R*)	C_8H_{15}	**25**	1.7 [1.6-1.8]	58 ± 3	84 ± 2
25	(2*R*,3*S*)	C_8H_{17}	**5**	1.7 [1.4–2.1]	47 ± 3	53 ± 3

IC_{50} values are given with 95% confidence intervals, CD98 and vacuolation scores are means ± SEM. $N \geqslant 3$ in all cases.

Table 2
Comparison of activities of *O*-alkyl pyrrolidine analogs

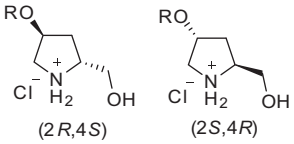

Entry	Compound; Stereochemistry	R	Compound number	IC_{50} (μM) [95% CI]	%CD98 down-regulation	Vacuolation score
1	FTY720		**1**	2.4 [2.1–2.7]	68 ± 3	82 ± 4
2	Sphingosine		**6**	3.6 [3.5–3.7]	48 ± 2	57 ± 6
3	Sphinganine		**7**	3.5 [3.3–3.7]	47 ± 3	38 ± 6
4	Dimethylsphingosine		**8**	0.8 [0.7–0.9]	69 ± 2	72 ± 3
5	C_2-Ceramide		**9**	33.0 [23.3–47.0]	47 ± 3	0
6	Dihydro-C_2-ceramide		**10**	Cytostatic	13 ± 4	0
7	(2*R*,4*S*)	$C_{12}H_{25}$	**26**	1.2 [1.1–1.3]	57 ± 2	53 ± 3
8	(2*R*,4*S*)	$C_{12}H_{23}$	**27**	2.6 [2.6-2.7]	34 ± 2	9 ± 5
9	(2*S*,4*R*)	$C_{12}H_{25}$	**28**	2.5 [2.4–2.6]	45 ± 3	36 ± 5
10	(2*S*,4*R*)	$C_{12}H_{23}$	**29**	3.3 [3.1–3.5]	30 ± 1	20 ± 4

IC_{50} values are given with 95% confidence intervals, CD98 and vacuolation scores are means ± SEM. $N \geqslant 3$ in all cases.

2, these activities were reversed and more transporter loss than vacuolation was observed (Fig. 4). When the hydrocarbon chain was saturated as in our previous reports[13,20], these differences in the ability to trigger nutrient transporter loss and vacuolation were present, but less apparent. For example, the (2*S*,4*R*) unsaturated compound **19** (Table 1 entry 17) triggers vacuolation twice as well as the (2*R*,4*S*) unsaturated enantiomer **13** (Table 1 entry 10), while the trend is reversed with **13** (Table 1 entry 10) which induces transporter loss nearly twice as much as **19** (Table 1 entry 17). These differential activities of enantiomeric compounds in

Table 3
Effect of N-substitution and unsaturation on the activities of *O*-benzyl and *C*-aryl pyrrolidine analogs

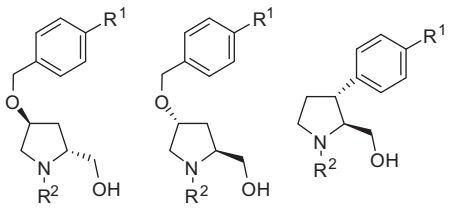

Entry	Compound; Stereochemistry	R^1	R^2	Compound number	IC50 (μM) [95% CI]	%CD98 down-regulation	Vacuolation score
1	FTY720			**1**	2.4 [2.1–2.7]	68 ± 3	82 ± 4
2	Sphingosine			**6**	3.6 [3.5–3.7]	48 ± 2	57 ± 6
3	Sphinganine			**7**	3.5 [3.3–3.7]	47 ± 3	38 ± 6
4	Dimethylsphingosine			**8**	0.8 [0.7–0.9]	69 ± 2	72 ± 3
5	C_2-Ceramide			**9**	33.0 [23.3–47.0]	47 ± 3	0
6	Dihydro-C_2-ceramide			**10**	Cytostatic	13 ± 4	0
	O-Benzyl series						
7	(2*R*,4*S*)	C_8H_{17}	H	**2**	2.0 [1.8–2.2]	63 ± 3	33 ± 2
8	(2*R*,4*S*)	C_8H_{15}	H	**13**	1.4 [1.3–1.6]	64 ± 1	27 ± 1
9	(2*S*,4*R*)	C_8H_{17}	H	**3**	3.0 [2.9–3.2]	48 ± 2	47 ± 2
10	(2*R*,4*S*)	C_8H_{15}	Me	**30**	1.9 [1.8–2.1]	31 ± 4	26 ± 2
11	(2*R*,4*S*)	C_8H_{17}	Ac	**31**	29.7 [ND]	37 ± 3	1 ± 1
12	(2*R*,4*S*)	C_8H_{17}	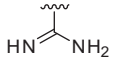	**32**	14.2 [12.5–16.1]	35 ± 1	0
13	(2*S*,4*R*)	C_8H_{17}	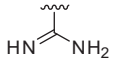	**33**	17.3 [15.9–18.9]	34 ± 3	0
	C-Aryl series						
14	(2*S*,3*R*)	C_8H_{17}	H	**4**	1.9 [1.8–2.1]	54 ± 1	81 ± 3
15	(2*S*,3*R*)	C_8H_{15}	H	**25**	1.7 [1.6–1.8]	58 ± 3	84 ± 2
16	(2*S*,3*R*)	C_8H_{17}	Ac	**34**	39.7 [37.1–42.4]	40 ± 4	0
17	(2*S*,3*R*)	C_8H_{15}	Ac	**35**	46.2 [43.5–49.0]	40 ± 2	2 ± 2

Effect of N-substitution and unsaturation on the activities of *O*-benzyl and *C*-aryl pyrrolidine analogs. IC_{50} values are given with 95% confidence intervals, CD98 and vacuolation scores are means ± SEM. $N \geqslant 3$ in all cases. ND, not determined due to solubility constraints.

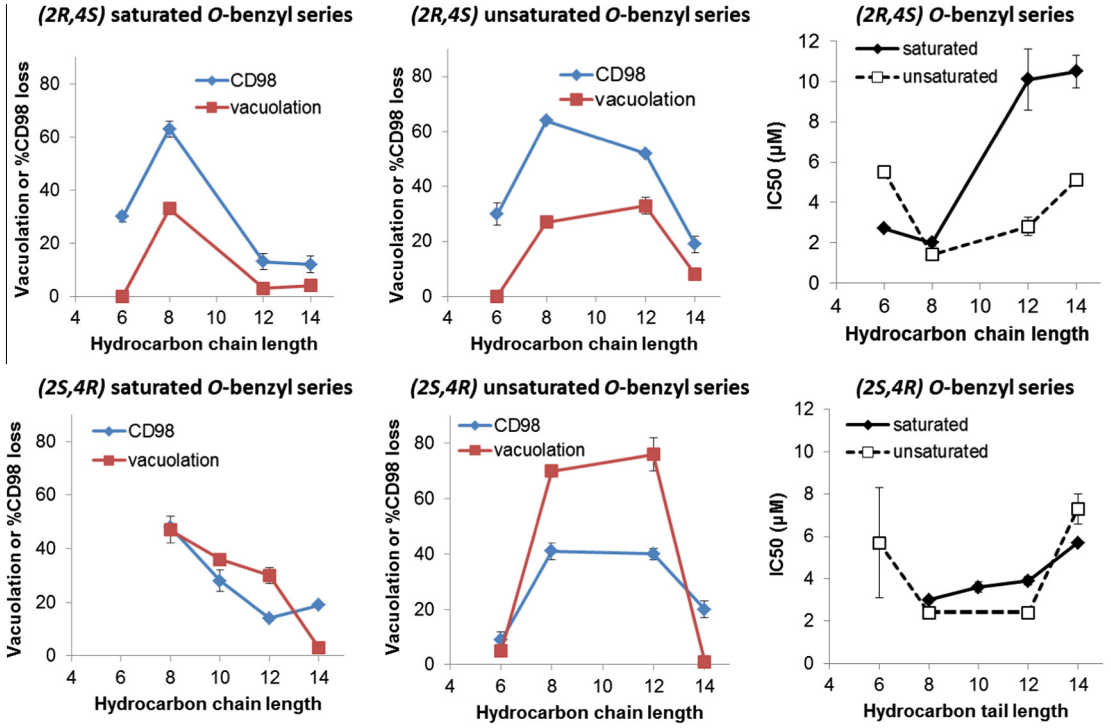

Figure 4. Effect of hydrocarbon tail length and saturation on vacuolation, transporter loss, and IC_{50}. Saturated and unsaturated compounds with the same stereochemistry are compared. All compounds were tested at 2.5 μM in vacuolation and transporter assays. Mean values are presented +/− SEM for transporter loss and vacuolation and with 95% CI for IC_{50}.

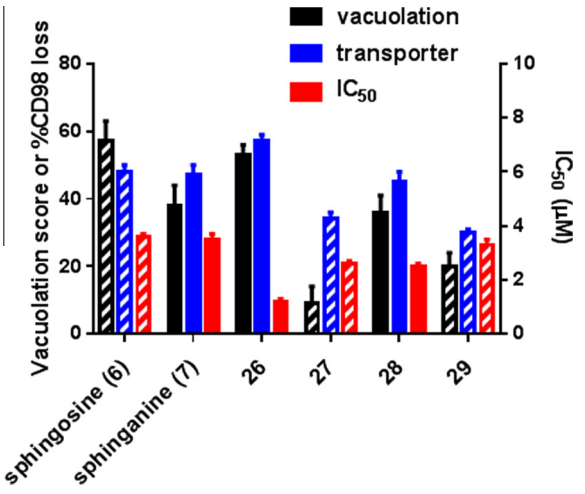

Figure 5. Effect of constraint on vacuolation, transporter loss, and cell killing by natural sphingolipids. All compounds were tested at 2.5 μM in vacuolation and transporter assays. Unsaturated compounds are shown with hatched bars. Mean values are presented +/− SEM for transporter loss and vacuolation and with 95% CI for IC_{50}.

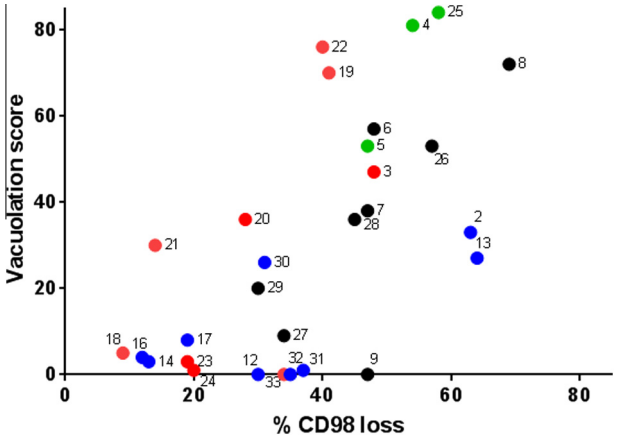

Figure 6. Comparison of vacuolation and transporter loss induced by the compounds under study. All compounds were tested at 2.5 μM except for C_2-ceramide (**9**, 50 μM), **31** (50 μM), and **32** and **33** (30 μM). *C*-Aryl compound are shown in green; *O*-benzyl compounds with (2*R*,4*S*) as in **2** are shown in blue, (2*S*,4*R*) stereochemistry as in **3** in red, and flexible or constrained natural sphingolipids in black. Mean values are plotted.

transporter and vacuolation assays are also apparent, but less robust, when the saturated compounds, **2** and **3** (Table 1 entry 9 and 13, respectively), are compared. The finding that enantiomers exhibit different if not reversed activity trends in these assays is significant because it could lead to the development of chemical biology tools to isolate the distinct targets responsible for these phenotypes. It is also interesting to note that the unsaturated (2*S*,4*R*) analogs of **3** are much more active in vacuolation assays than the matched saturated compounds. Partial unsaturation increases transporter loss as well, but to a lesser degree. Because unsaturation in the hydrocarbon chain increased the activity of all compounds in each assay, we evaluated whether unsaturation would also enhance the activity of the structurally related *C*-aryl series as in (2*S*,3*R*) **4** (Fig. 1 and Table 1, entry 23). Analog **25** (Table 1, entry 24) was not significantly more active than its saturated counterpart **4** (Table 1, entry 23) in any of the assays. However, **4** (Table 1, entry 23) is much better at inducing vacuolation than the corresponding saturated *O*-benzyl, **3** (Table 1, entry 16) analog. As in the *O*-benzyl series, we observe a stereochemical dependence for optimal activity within the *C*-aryl series. Thus, the *C*-aryl analog (2*R*,3*S*) **5** (Table 1, entry 25) does not vacuolate as well as the enantiomeric (2*S*,3*R*) **4** (Table 1, entry 23) with scores of 53 and 81, respectively. To summarize the conclusions drawn from SAR studies with the compounds in Table 1, the (2*S*,4*R*) stereochemistry in the *O*-benzyl series represented by **3** leads to better vacuolation, while the enantiomeric (2*R*,4*S*) stereochemistry as in **2** promotes nutrient transporter down-regulation (Table 1 entries 16 and 9, respectively). These results could reflect differential affinities for distinct PP2A heterotrimers. The C8 hydrocarbon chain length is favored in both assays, and, at this optimal tail length, unsaturation has only a minor positive effect on activity. Better vacuolation is observed with the *C*-aryl (2*S*,3*R*) and (2*R*,3*S*) analogs **4** and **5** compared to the *O*-benzyl counterparts **3** and **2**, respectively.

We next considered 2-hydroxymethyl pyrrolidine versions of sphingosine (**6**) and sphinganine (**7**) except that the aromatic moiety in the original series represented by **2** and **3** was replaced by hydrocarbon chains of varying degrees of saturation and unsaturation as 3-*O*-ethers (Fig. 2). Replacing the polar amino diol portion of sphingosine (**6**) and sphinganine (**7**) with a pyrrolidine ring did not dramatically alter the IC_{50} values of the enantiomeric analogs **26**–**29** with the exception that **26** was 3-fold more cytotoxic than the parent compound, sphinganine (**7**, Table 2, Fig. 5). CD98 transporter loss and vacuolation were slightly greater with **26** (Table 2 entry 7) than with the parent sphinganine (**7**, Table 2 entry 3), consistent with its increased cytotoxicity. However, the unsaturated analog **27** (Table 2 entry 8) exhibited decreased activity in transporter and vacuolation assays compared to sphingosine (**6**, Table 2 entry 2) without a concomitant increase in the IC_{50}. Sphingosine (**6**) and sphinganine (**7**) have similar effects on nutrient transporter proteins, however sphingosine (**6**) vacuolates much better than sphinganine (**7**) (Fig. 3). Surprisingly, this relationship was reversed in the constrained analogs, where the enantiomeric fully saturated constrained sphinganine analogs **26** and **28** were 2–4-fold more active in vacuolation assays than the unsaturated sphingosine analogs **27** and **29** (Table 2 entries 7–10).

Stereochemistry had a only a modest effect in this series, although the (2*R*,4*S*) stereoisomers were slightly better at vacuolation than the (2*S*,4*R*) versions (Table 2, entries 7–10, Fig. 5). In summary, unlike in the *O*-benzyl series, constraint had a negative effect on the transporter and vacuolation activities of sphingosine (**6**) but not sphinganine (**7**).

One of the key goals of this study was to determine the structural features that influence activation of the disparate targets involved in nutrient transporter loss and vacuolation. C_2-Ceramide (**9**), which differs from sphingosine (**6**) by the acetylation of its amino group (Fig. 2), induces nutrient transporter loss but not vacuolation at concentrations above its IC_{50} (Fig. 3). We were cognizant that reducing the basic character of the pyrrolidine nitrogen atom in analogs such as **2**, **3**, and **4** by *N*-acetylation should result in greatly diminished activity in transporter and cytotoxicity assays based on previous results with the corresponding lactams.[13,20] However, the effects of such a modification on vacuolation were unknown. As expected, given the lack of the basic nitrogen, *N*-acetyl analog **31** in the *O*-benzyl series (Table 3 entry 11) was 10-fold less potent than **2**, in analogy with the similar difference in potency between C_2-ceramide (**9**) and sphingosine (**6**) (Table 3 entries 2 and 5). Furthermore, analog **31** exhibited no vacuolation activity at the highest dose tested (Table 3 entry 11). The effect of *N*-acetylation on *C*-aryl compounds such as **4** and **25** which induce vacuolation very efficiently was also evaluated Although loss of transporter activity was not as significant, compounds **34** and **35** also failed to induce vacuolation, (Table 3 entries 16 and 17). Thus, *N*-acetylated pyrrolidine FTY720 analogs in the

C-aryl series as reported here may be useful as chemical biology tools to isolate and identify the individual targets responsible for transporter loss and vacuolation.

A second goal of these SAR studies was to identify functional characteristics in constrained FTY720 analogs that would maintain potency while effecting transporter loss and efficient vacuolation, thereby contributing to cancer cell death. The finding that *N*-acetylation reduces potency is consistent with our previous observations that the positive charge of the nitrogen in the pyrrolidine is critical for enhanced compound activity.[13,20] Since dimethylsphingosine (**8**) exhibited the best potency, transporter loss and vacuolation among the sphingolipids tested (Tables 1–3, Fig. 3), we surmised that the *N*-methyl analog **30** would represent a good mimic, albeit with a pyrrolidine scaffold. Interestingly, the *N*-methyl analog **30** was not more active than the parent **13**, and its ability to induce transporter loss and vacuolation were reduced (Table 3, entries 8 and 10). To determine whether increasing the basicity of the pyrrolidine nitrogen atom would also increase potency, we generated guanidino analogs **32** and **33** (Table 3). However, the potency of these compounds was reduced 5–7 fold compared to the parent compounds **3** and **2** in the same series (Table 3, entries 12 and 13). Moreover, the ability to induce vacuole formation was lost even at the highest concentrations tested (30 μM). These results suggest that although basicity is important, steric effects in the environment of the pyrrolidine nitrogen may play a role in interactions with cellular targets.

3. Conclusion

In summary, these SAR studies of constrained anti-cancer FTY720 pyrrolidine analogs suggest that a compound with an unsaturated C8 hydrocarbon chain in the (2*S*,4*R*)-*O*-benzyl pyrrolidine series such as **19** will have higher overall activity than saturated, longer or shorter chain analogs having the same stereochemistry (Fig. 6). The (*S*,*R*) stereochemistry as in **19** correlates with better vacuolating ability while the enantiomeric (*R*,*S*) compounds, as in **2** and **13**, are slightly better at triggering nutrient transporter loss (Table 1 and Figs. 4 and 6). However, in the *C*-aryl series, this difference in transporter down- regulation between enantiomers becomes negligible (54% vs 47% with **4** and **5**, respectively). Of the pyrrolidine analogs tested, the saturated and unsaturated *C*-aryl analogs **4** and **25**, respectively are the most potent inducers of vacuolation and transporter loss leading to potent cytotoxicity in the low μM range (Fig. 6). Given this profile, these compounds would be predicted to have the highest anti-tumor activity in vivo in this series of constrained FTY720 analogs. Indeed, **4** exhibits activity against both colon cancer and prostate cancer in animal models.[13,22] Furthermore, these compounds fail to activate the undesirable S1P receptor which is known to dramatically reduce heart rate. As a result of this study, we identified several compounds such as **34** and **35** that might provide valuable chemical biology tools to isolate the distinct targets involved in vacuolation and transporter down-regulation. For example, while C_2-ceramide (**9**) shows good activity in transporter down-regulation assays among the non-vacuolating sphingolipids (Fig. 6), it is rapidly metabolized and therefore less suitable as a chemical probe than synthetic, constrained versions that are likely to be less readily metabolized by cellular enzymes. Thus, compounds **12** or **31**–**35**, lacking any vacuolating activity, would likely be superior ligands for selective isolation of the target(s) involved in nutrient transporter loss. No compounds were identified that cause vacuolation without also triggering transporter loss (Fig. 6). Therefore, comparing this dataset to proteins isolated by compounds with similar transporter down-regulation abilities that also vacuolate well such as **22** and **19** could permit identification of protein targets responsible for vacuolation. Future studies will address the deconvolution of these targets.

Acknowledgements

SH thanks NSERC for financial assistance. This work was supported by grants to ALE from the NIH (R01 GM089919, R21 CA178230), CDMRP (W81XWH-11-1-0535 and W81XWH-15-1-0010), the American Cancer Society (RSG-11-111-01-CDD), and the UCI CORCL.

Supplementary data

Supplementary data (synthesis details of all intermediates and final compounds, biological procedures, ^{1}H and ^{13}C spectra, and HPLC analysis) associated with this article can be found, in the online version, at http://dx.doi.org/10.1016/j.bmc.2016.07.038.

References and notes

1. Skrzypek, M. S.; Nagiec, M. M.; Lester, R. L.; Dickson, R. C. *J. Biol. Chem.* **1998**, *273*, 2829.
2. Welsch, C. A.; Roth, L. W.; Goetschy, J. F.; Movva, N. R. *J. Biol. Chem.* **2004**, *279*, 36720.
3. Selwan, E. M.; Finicle, B. T.; Kim, S. M.; Edinger, A. L. *FEBS Lett.* **2016**, *590*, 885.
4. Guenther, G. G.; Peralta, E. R.; Rosales, K. R.; Wong, S. Y.; Siskind, L. J.; Edinger, A. L. *Proc. Natl. Acad. Sci. U.S.A.* **2008**, *105*, 17402.
5. Guenther, G. G.; Liu, G.; Ramirez, M. U.; McMonigle, R. J.; Kim, S. M.; McCracken, A. N.; Joo, Y.; Ushach, I.; Nguyen, N. L.; Edinger, A. L. *Oncogene* **2014**, *33*, 1776.
6. Romero Rosales, K.; Singh, G.; Wu, K.; Chen, J.; Janes, M. R.; Lilly, M. B.; Peralta, E. R.; Siskind, L. J.; Bennett, M. J.; Fruman, D. A.; Edinger, A. L. *Biochem. J.* **2011**, *439*, 299.
7. Welsch, C. A.; Hagiwara, S.; Goetschy, J. F.; Movva, N. R. *J. Biol. Chem.* **2003**, *278*, 26976.
8. Feun, L. G.; Kuo, M. T.; Savaraj, N. *Curr. Opin. Clin. Nutr. Metab. Care* **2015**, *18*, 78.
9. Jain, M.; Nilsson, R.; Sharma, S.; Madhusudhan, N.; Kitami, T.; Souza, A. L.; Kafri, R.; Kirschner, M. W.; Clish, C. B.; Mootha, V. K. *Science* **2012**, *336*, 1040.
10. Maddocks, O. D.; Berkers, C. R.; Mason, S. M.; Zheng, L.; Blyth, K.; Gottlieb, E.; Vousden, K. H. *Nature* **2013**, *493*, 542.
11. Azuma, H.; Takahara, S.; Horie, S.; Muto, S.; Otsuki, Y.; Katsuoka, Y. *J. Urol.* **2003**, *169*, 2372.
12. Azuma, H.; Takahara, S.; Ichimaru, N.; Wang, J. D.; Itoh, Y.; Otsuki, Y.; Morimoto, J.; Fukui, R.; Hoshiga, M.; Ishihara, T.; Nonomura, T.; Suzuki, S.; Okuyama, A.; Katsuoka, Y. *Cancer Res.* **2002**, *62*, 1410.
13. Chen, B.; Roy, S. G.; McMonigle, R. J.; Keebaugh, A.; McCracken, A. N.; Selwan, E.; Fransson, R.; Fallegger, D.; Huwiler, A.; Kleinman, M. T.; Edinger, A. L.; Hanessian, S. *ACS Chem. Biol.* **2016**, *11*, 409.
14. Chua, C. W.; Lee, D. T.; Ling, M. T.; Zhou, C.; Man, K.; Ho, J.; Chan, F. L.; Wang, X.; Wong, Y. C. *Int. J. Cancer* **2005**, *117*, 1039.
15. Neviani, P.; Santhanam, R.; Oaks, J. J.; Eiring, A. M.; Notari, M.; Blaser, B. W.; Liu, S.; Trotta, R.; Muthusamy, N.; Gambacorti-Passerini, C.; Druker, B. J.; Cortes, J.; Marcucci, G.; Chen, C. S.; Verrills, N. M.; Roy, D. C.; Caligiuri, M. A.; Bloomfield, C. D.; Byrd, J. C.; Perrotti, D. *J. Clin. Invest.* **2007**, *117*, 2408.
16. Camm, J.; Hla, T.; Bakshi, R.; Brinkmann, V. *Am. Heart J.* **2014**, *168*, 632.
17. Cohen, J. A.; Chun, J. *Ann. Neurol.* **2011**, *69*, 759.
18. Koyrakh, L.; Roman, M. I.; Brinkmann, V.; Wickman, K. *Am. J. Transp.* **2005**, *5*, 529.
19. Schmouder, R.; Serra, D.; Wang, Y.; Kovarik, J. M.; DiMarco, J.; Hunt, T. L.; Bastien, M. C. *J. Clin. Pharmacol.* **2006**, *46*, 895.
20. Fransson, R.; McCracken, A. N.; Chen, B.; McMonigle, R. J.; Edinger, A. L.; Hanessian, S. *ACS Med. Chem. Lett.* **2013**, *4*, 969.
21. Hanessian, S.; Charron, G.; Billich, A.; Guerini, D. *Bioorg. Med. Chem. Lett.* **2007**, *17*, 491.
22. Kim, S. M.; Roy, S. G.; Chen, B.; Nguyen, T.; McMonigle, R. J.; McCracken, A. N.; Zhang, Y.; Kofuji, S.; Selwan, E.; Finicle, B. T.; Nguyen, T.; Ravi, A.; Ramirez, M. U.; Wiher, T.; Guenther, G. G.; Kono, M.; Sasaki, A. T.; Weisman, L. S.; Potma, E. O.; Tromberg, B. J.; Edwards, R. A.; Hanessian, S.; Edinger, A. L. resubmission under review.
23. McCracken, A. N.; McMonigle, R. J.; Tessier, J.; Fransson, R.; Perryman, M. S.; Chen, B.; Keebaugh, A.; Selwan, E.; Barr, S. A.; Kim, S. M.; Roy, S. G.; Fallegger, D.; Brandt, C.; Moitessier, N.; Snider, A. J.; Clare, S.; Muschen, M.; Huwiler, A.; Kleinman, M. T.; Hanessian, S.; Edinger, A. L. submitted.
24. Chalfant, C. E.; Szulc, Z.; Roddy, P.; Bielawska, A.; Hannun, Y. A. *J. Lipid Res.* **2004**, *45*, 496.
25. Dobrowsky, R. T.; Kamibayashi, C.; Mumby, M. C.; Hannun, Y. A. *J. Biol. Chem.* **1993**, *268*, 15523.
26. Haberkant, P.; Stein, F.; Hoglinger, D.; Gerl, M. J.; Brugger, B.; Van Veldhoven, P. P.; Krijgsveld, J.; Gavin, A. C.; Schultz, C. *ACS Chem. Biol.* **2016**, *11*, 222.

27. Habrukowich, C.; Han, D. K.; Le, A.; Rezaul, K.; Pan, W.; Ghosh, M.; Li, Z.; Dodge-Kafka, K.; Jiang, X.; Bittman, R.; Hla, T. *J. Biol. Chem.* **2010**, *285*, 26825.
28. Cristobal, I.; Madoz-Gurpide, J.; Manso, R.; Gonzalez-Alonso, P.; Rojo, F.; Garcia-Foncillas, J. *Curr. Med. Res. Opin.* **2016**, 1.
29. Oaks, J.; Ogretmen, B. *Front. Oncol.* **2014**, *4*, 388.
30. Sents, W.; Ivanova, E.; Lambrecht, C.; Haesen, D.; Janssens, V. *FEBS J.* **2013**, *280*, 644.
31. Obeid, L. M.; Linardic, C. M.; Karolak, L. A.; Hannun, Y. A. *Science* **1993**, *259*, 1769.